Stabilization of a β-Hairpin Conformation in a Cyclic Peptide Using the Templating Effect of a Heterochiral Diproline Unit

by **Julia Späth**, **Fiona Stuart**, **Luyong Jiang**, and **John A. Robinson***

Institute of Organic Chemistry, University of Zürich, Winterthurerstrasse 190, CH-8057 Zürich

A straightforward and effective method of stabilizing a β-hairpin conformation in a cyclic protein loop mimetic is described, which exploits the templating effect of a heterochiral D-Pro-L-Pro dipeptide unit. A twelve-residue β-hairpin loop was grafted from the extracellular interferon γ receptor onto the heterochiral D-Pro-L-Pro dipeptide template to afford a fourteen-residue cyclic peptide. The residues directly attached to the D-Pro-L-Pro template are shown by NMR spectroscopy to structurally mimic corresponding residues in adjacent antiparallel β-strands in the receptor. MD Simulations with and without time-averaged distance restraints support this view and indicate that the tip of the loop is more flexible, as inferred also for the receptor protein from crystallographic data. The templating effect of the heterochiral diproline unit also promotes efficient backbone cyclization of the fourteen-residue linear peptide precursor, suggesting that a wide variety of related protein loop mimetics incorporating the D-Pro-L-Pro template might be readily accessible.

1. Introduction. – There is growing interest in the use of structure-function-based design methods to mimic, in small synthetic molecules, interactions that occur at large protein-protein interfaces [1]. In this regard, loops on the surface of proteins involved in recognition are an interesting target for mimetic design. Antigen binding sites on antibodies, and ligand binding sites on cytokine receptors, *e.g.*, comprise up to six recognition loops that extend from the core of a β-sheet protein. We report here attempts to prepare mimics of an antiparallel β-sheet loop on the extracellular interferon γ receptor (IFNγR) involved in binding the natural ligand IFNγ [2], and a neutralizing monoclonal antibody A6 [3], using cyclic peptides constrained by a heterochiral D-Pro-L-Pro dipeptide template (see **1a** and **1b**).

The loop of interest comprises residues Lys^{47} to Trp^{56}, which connect adjacent strands of a β-sheet in the N-terminal Ig-like domain of the IFNγR. This domain comprises two antiparallel β-sheets composed of strands A, B, and E, and G, F, C, and C′, as depicted in *Fig. 1*. The residues Val^{46} and Ile^{57} lie within the β-sheet, with their side chains buried in the hydrophobic interior of the protein (*Fig. 2*), whereas the intervening residues comprise the exposed CC′ recognition loop. The approach taken here to generate a mimetic of the CC′ loop involved transplanting the sequence Val^{46} to Ile^{57} from the protein onto a template whose geometry would fix, in particular, the end residues (*i.e.*, Val^{46}-Lys^{47} and Trp^{56}-Ile^{57}) in the same geometry found in the intact receptor. We show that a heterochiral D-Pro-L-Pro, in the context of a cyclic peptide (see **1a,b**), functions admirably as a template to stabilize a β-hairpin-loop conformation in aqueous solution. For comparison, the disulfide-bridged loop **2** is shown to be significantly more flexible.

The β-turn-inducing properties of a D-Pro-L-Pro dipeptide unit are well-known. *Kopple* and coworkers [4] demonstrated that the D-Pro-L-Pro sequence exhibits a

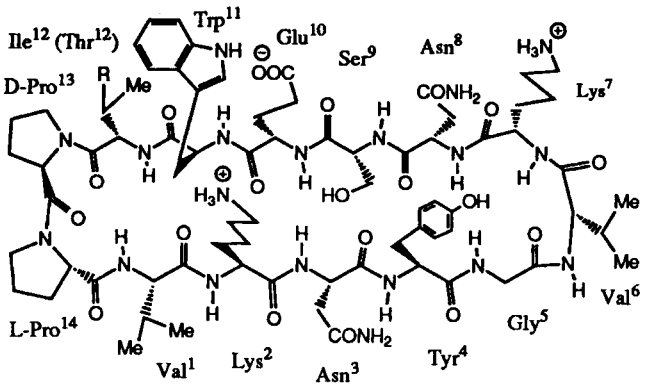

1a R = Et (Ile[12])
b R = OH (Thr[12])

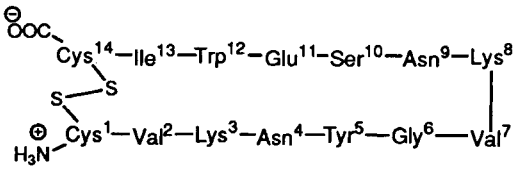

2

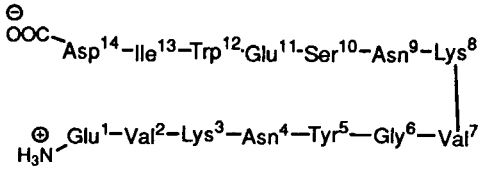

3

strong preference for a type-II′ β-turn conformation, and can be used to fix β-turn positions in cyclic hexapeptides. A crystal structure [5] of pivaloyl-D-Pro-L-Pro-L-Ala-NHMe revealed a similar type-II′ β-turn conformation. *Marshall* and coworkers [6] used conformational search methods to show that a type-II′ β-turn is strongly favoured by D-Pro-L-Pro, whereas L-Pro-L-Pro and D-Pro-D-Pro are poorer turn-constraining units due to enhanced *cis-trans* isomerism and the small energy differences between turn-like and extended structures. Applications of the D-Pro-L-Pro dipeptide unit in receptor-ligand design [7], and of substituted analogs as β-turn-forming peptidomimetics [8], have also been reported. Our results are consistent with those of earlier conformational studies and point out, in particular, the templating effect of a D-Pro-L-Pro unit and its use to stabilize β-hairpin conformations. We also show that a D-Pro-L-Pro unit incorporated during synthesis near the middle of a linear peptide chain promotes efficient cyclization of the peptide backbone; thus, simple and efficient access to a general class of cyclic protein loop mimetics of this type appears feasible, possibly also using combinatorial chemistry methods.

2. Results and Discussion. – 2.1. *Synthesis.* The relevant sequence of the IFNγR comprises Glu[45]-Val[46]-Lys[47]-Asn[48]-Tyr[49]-Gly[50]-Val[51]-Lys[52]-Asn[53]-Ser[54]-Glu[55]-Trp[56]-Ile[57]-

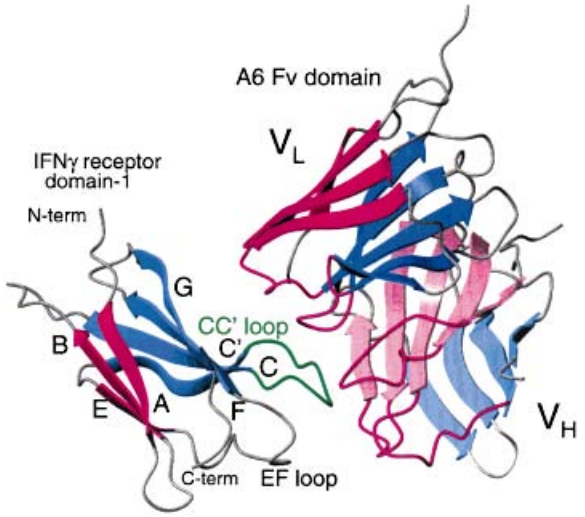

Fig. 1. *Ribbon diagram* [18] *of the* F_V *region* ($V_H + V_L$) *of A6 Fab bound to the N-termianl Ig-like domain of the extracellular IFNγR, as determined by crystallography* [3]. The CC′ loop and the seven β-strands of the fibronectin type-III fold are indicated (A–C, C′, E–G). The antibody complementarity determining regions (CDRs) are in red.

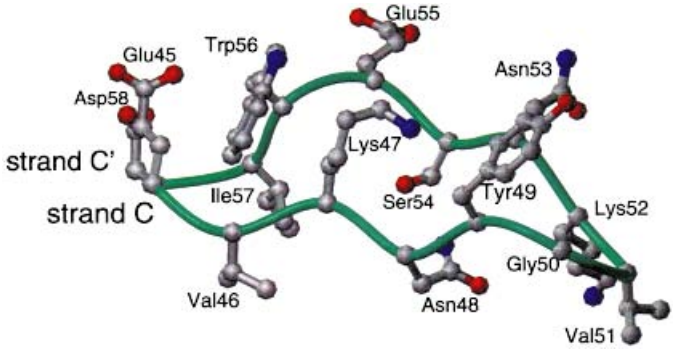

Fig. 2. *Ribbon representation of the CC′ loop of the IFNγR with ball-and-stick models of the C(α) atoms and the side chains of residues* Glu^{45} *to* Asp^{58}. O-Atoms in red, N-atoms in blue and C-atoms in grey. Same orientation as in *Fig. 1*.

Asp^{58}, with residues of the CC′ loop important for ligand recognition being Lys^{57} to Trp^{56} (*Fig. 2*). A linear peptide of the same sequence, *i.e.*, **3**, was prepared by solid-phase methods using Fmoc chemistry [9]. A loop conformation was constrained in **2** by a disulfide bridge, which was introduced after assembly of the linear peptide precursor, also by Fmoc chemistry. The cysteine residues were introduced by formal replacement of Glu^{45} and Asp^{58} in the linear epitope.

The linear precursors of mimetics **1a** and **1b** were synthesized on a solid phase, starting with the Gly^5 residue, and then cleaved from the resin with 1% CF_3COOH in CH_2Cl_2 without removal of side-chain-protecting groups. Cyclization between Gly^5 and

Val[6] was performed in solution with HATU and HOAt[1]). All side-chain-protecting groups were then removed, and the products were purified by HPLC. The high efficiency of the cyclizations is notable, as evidenced by HPLC of the side-chain-protected linear peptide precursor of **1b** before, and the product directly after cyclization (*Fig. 3*).

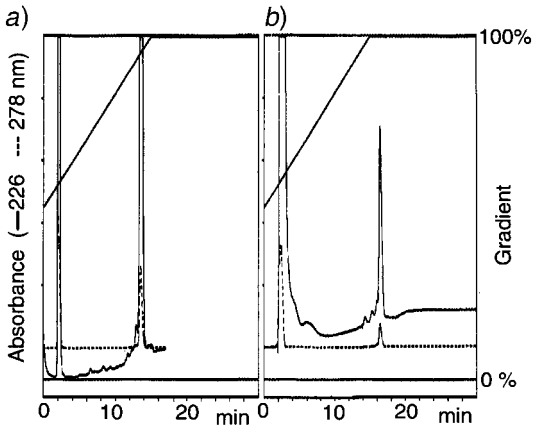

Fig. 3. *HPLC of* a) *the linear protected precursor of* **1b** *and* b) *after cyclization* (the sample was taken directly from the reaction in DMF, before workup). C_{18}-Reversed-phase column (*Waters*; 100 × 8 mm), gradient of 50–100% MeCN with H_2O + 0.1% of CF_3COOH.

2.2. *NMR and MD Studies.* 2.2.1. *General.* The ^{1}H-NMR spectra of peptides **1**–**3** were measured in H_2O D_2O 9:1 at pH 5, using standard methods [10] . Only the spectral properties of **1b** are presented in detail, with reference, where appropriate, to those of **1a**, **2**, and **3**. The ^{1}H-NMR spectra of **1a** and **1b** revealed a major set of resonances, and two minor ones, in the ratio 88 : 8.5 : 3.5. No exchange cross-peaks were seen in ROESY spectra at 300 K. Both peptides appeared homogeneous by anal. HPLC. The minor components may represent *cis-trans* conformers at X-Pro peptide bonds that interconvert slowly on the NMR time scale. The minor species were not investigated further due to problems of spectral overlap.

The peptide **1a** corresponds to the natural sequence of the receptor loop (Val[46] to Ile[57]) mounted on the D-Pro-L-Pro template. However, several H–C(α) resonances overlap in aqueous solution, which made the unambiguous assignment of several NOEs impossible. This problem was largely overcome in peptide **1b**, which was used for more detailed studies. Evidence for stable secondary structure in **1b** was first sought through an analysis of chemical shifts, amide temperature coefficients, H/D exchange rates, and NOEs.

2.2.2. *Chemical Shifts and Coupling Constants.* The ^{1}H-NMR chemical shift assignments for **1b** at 285 K given in *Table 1* were invariant over the concentration range 0.1–30 mM. Deviations from random-coil shifts [11] in water at pH 5.0 and 285 K were observed, in particular for the Thr[12] NH resonance which is shifted 0.7 ppm

[1]) Abbreviations. HOAt, 1-hydroxy-7-azabenzotriazole (= 1-hydroxy-1*H*-1,2,3-triazolo[4,5-*b*]pyridine); HATU, *O*-(7-azabenzotriazol-1-yl)-*N*,*N*,*N*′,*N*′-tetramethyluronium hexafluorophosphate = *O*-(1*H*-1,2,3-triazolo[4,5-*b*]pyridin-1-yl)-*N*,*N*,*N*′,*N*′-tetramethyluronium hexafluorophosphate.

downfield from the random-coil value. On the other hand, the Lys[2] side-chain resonances are unusually high-field shifted (*e.g.*, $CH_2(\gamma)$ at 0.32 and 0.53 ppm), due to close proximity to the indole ring of Trp[11] (see below). The same effects are seen in the spectra of **1a**, but not in those of **2** (*Table 2*).

Table 1. *^{1}H-NMR* (600 MHz) *Chemical Shifts for* **1b** *at 285 K in 10% $^2H_2O/H_2O$ at pH 5.0*

Residue	Chemical shift [ppm] [a])			
	NH	H–C(α)	H–C(β) [b])	others [b]) [c])
Val[1]	7.82	4.17	2.13	0.97, 0.89 ($CH_3(\gamma)$)
Lys[2]	8.28	3.66	1.09, 0.61	0.32, 0.53 ($CH_2(\gamma)$); 1.01 ($CH_2(\delta)$); 2.55 ($CH_2(\varepsilon)$)
Asn[3]	8.08	4.64	2.61, 2.66	7.38 ($NH(\delta)^E$); 6.91 ($NH(\delta)^Z$)
Tyr[4]	8.45	4.43	3.02, 2.85	7.09 (CH(δ)); 6.78 (CH(ε))
Gly[5]	8.36	3.95, 3.83	–	–
Val[6]	7.92	4.13	2.09	0.91, 0.93 ($CH_3(\gamma)$)
Lys[7]	8.52	4.21	1.78	1.39 ($CH_2(\gamma)$); 1.64 ($CH_2(\delta)$); 2.97 ($CH_2(\varepsilon)$)
Asn[8]	8.30	4.52	2.78	7.63 ($NH(\delta)^E$); 6.98 ($NH(\delta)^Z$)
Ser[9]	8.10	4.45	3.88, 3.80	–
Glu[10]	8.47	4.34	2.03, 1.95	2.27, 2.17 ($CH_2(\gamma)$);
Trp[11]	8.48	4.88	2.97, 3.48	7.20 (H–C(2), H–C(6)); 7.51 (H–C(4)); 7.04 (H–C(5)); 7.44 (H–C(7)); 10.05 (NH)
Thr[12]	9.16	4.81	4.16	1.22 ($CH_3(\gamma)$)
D-Pro[13]	–	4.77	2.31, 1.87	2.12, 2.02 ($CH_2(\gamma)$); 3.90, 3.57 ($CH_2(\delta)$)
L-Pro[14]	–	4.62	2.23	2.12, 1.97 ($CH_2(\gamma)$); 3.97, 3.73 ($CH_2(\delta)$)

[a]) Chemical shifts are measured relative to internal TSP (sodium 3-(trimethylsilyl)($^2H_4$)propanoate). [b]) Stereospecific assignments are not available. [c]) The superscripts *E* and *Z* refer to the *trans* and *cis* relationship, respectively, of *H*–N(δ) and *O*–C(γ).

Table 2. *^{1}H-NMR* (600 MHz) *Chemical Shifts for* **2** *at 300 K in 10% $^2H_2O/H_2O$ at pH 5.0*

Residue	Chemical shift [ppm] [a])			
	NH	H–C(α)	H–C(β) [b])	others [b]) [c])
Cys[1]	–	4.49	3.18	–
Val[2]	8.15	4.32	2.09	0.94 ($CH_3(\gamma)$)
Lys[3]	8.31	4.09	1.40	1.06, 0.97 ($CH_2(\gamma)$); 1.40 ($CH_2(\delta)$); 2.73 ($CH_2(\varepsilon)$)
Asn[4]	8.21	4.67	2.73, 2.55	7.50 ($NH(\delta)^E$); 6.86 ($NH(\delta)^Z$)
Tyr[5]	8.28	4.46	3.06, 2.89	7.10 (CH(δ)); 6.81 (CH(ε))
Gly[6]	8.31	3.90	–	–
Val[7]	7.76	4.15	2.09	0.93, 0.90 ($CH_3(\gamma)$)
Lys[8]	8.43	4.23	1.81, 1.74	1.41, 1.36 ($CH_2(\gamma)$); 1.65 ($CH_2(\delta)$); 2.97 ($CH_2(\varepsilon)$)
Asn[9]	8.34	4.55	2.78	7.54 ($NH(\delta)^E$); 6.90 ($NH(\delta)^Z$)
Ser[10]	8.11	4.36	3.88, 3.79	–
Glu[11]	8.33	4.31	1.97, 1.85	2.17, 2.09 ($CH_2(\gamma)$)
Trp[12]	8.10	[d])	3.25, 3.16	7.21 (H–C(2)); 7.23 (H–C(6)); 7.50 (H–C(4)); 7.12 (H–C(5)); 7.48 (H–C(7)); 10.06 (NH)
Ile[13]	8.26	4.29	1.85	0.93 ($CH_3(\gamma)$); 1.41, 1.10 ($CH_2(\gamma)$); 0.82 ($CH_3(\delta)$)
Cys[14]	8.16	4.51	3.23, 3.02	–

[a]) Chemical shifts are measured relative to internal TSP (sodium 3-(trimethylsilyl)($^2H_4$)propanoate). The ^{1}H-NMR spectrum showed a single species on the chemical-shift time scale. [b]) Stereospecific assignments are not available. [c]) The superscripts *E* and *Z* refer to the *trans* and *cis* relationship, respectively, of *H*–N(δ) and *O*–C(γ). [d]) The signal lies under the water peak.

The $^3J(\alpha,NH)$ coupling constants of Val[1] and Thr[12] of **1b** are *ca.* 9 Hz (*Table 3*), which is consistent with a β-conformation. The $^3J(\alpha,\beta)$ coupling constants of Trp[11] have high and low values indicating a single preferred side-chain conformation. The other $^3J(\alpha,NH)$ coupling constants given in *Table 3*, however, are closer to random-coil values and are suggestive of varying degrees of conformational averaging.

Table 3. *Temperature Coefficients*[a]) ($-\Delta\delta/T$ [ppb/K]) *and H/D Exchange Rates*[b]) ($t_{1/2}$ [min]) *for Amide Protons and* ^{3}J *Coupling Constans*[c]) [Hz] *Measured for* **1b**

Residue	Val[1]	Lys[2]	Asn[3]	NH^{E}[d])	NH^{Z}[d])	Tyr[4]	Gly[5]	Val[6]	Lys[7]
$-\Delta\delta/T$ [ppb/K]	2.3	9.7	3.2	2.2	4.4	8.8	4.8	8.2	7.6
H/D $t_{1/2}$ [min]	82	19	6	r	r	6	r	r	r
$^3J(\alpha,NH)$ [Hz]	8.9	7.2	8.3	–	–	7.0	5.0, 6.0	7.0	6.1
$^3J(\alpha,\beta)$ [Hz]	9.0	8.4, 6.3	8.3, 5.5	–	–	9.0, 5.5	–	6.9	9.0, 5.6

Residue	Asn[8]	NH^{E}[d])	NH^{Z}[d])	Ser[9]	Glu[10]	Trp[11]	Thr[12]	Pro[13]	Pro[14]
$-\Delta\delta/T$ [ppb/K]	5.9	6.5	6.0	5.2	8.0	8.0	10.1	–	–
H/D $t_{1/2}$ [min]	r	r	r	r	15		43	–	–
$^3J(\alpha,NH)$ [Hz]	7.2	–	–	7.2	7.0	7.5	9.5	–	–
$^3J(\alpha,\beta)$ [Hz]	7.0, 5.6	–	–	6.0, 5.0	9.7, 5.5	11.0, 3.0	7.1	8.3, 6.2	6.0, 5.0

[a]) The temperature coefficients for the peptide amides and the side-chain NHs of Asn are given. Measurements were made in aqeuous solution (10% $^2H_2O/H_2O$, pH 5) in the range 280–300 K. [b]) The half-lives ($t_{1/2}$ [min]) of amide resonances were determined by fitting residual peak intensities after dissolution in D_2O (pD* 3.5, 300 K) to an exponential function; r indicates that the NH signal was completely exchanged before sufficient data points could be measured to determine half-lives; the residual signal for Glu[10]/Trp[11] could not be assigned unambiguously and could refer to either, or the sum of both, resonances (the signal decay fitted well a monoexponential function). [c]) Measured in 1D and/or E. COSY spectra. [d]) Side-chain NHs of Asn[3] and Asn[8], respectively. The superscripts *E* and *Z* refer to the *trans* and *cis* relationship, respectively, of $H-N(\delta)$ and $O-C(\gamma)$.

2.2.3. *Amide Temperature Coefficients and H/D Exchange Rates.* The backbone NH and side-chain NH groups of **1b** show linear changes in chemical shift with temperature in the range studied. The temperature coefficients are given in *Table 3*. In addition, six of the NH groups exchange sufficiently slowly for the rates to be measured by following the disappearance of the NH resonance after dissolution in D_2O at pD* 3.5 at 300 K. As given in *Table 3*, the Val[1]NH and Thr[12]NH flanking the D-Pro-L-Pro template exchanged relatively slowly, consistent with their involvement in intramolecular H-bonding. However, a relatively slow NH exchange does not always correlate with a low temperature coefficient (see, *e.g.*, Thr[12] NH, *Table 3*). In the case of **2**, the Val[7], Trp[12], and Val[2] backbone NHs showed the longest half-lives at 6, 11, and 23 min, respectively, at pD* 3.5 and 300 K.

2.2.4. *NOEs.* NOESY and ROESY data of **1b** at both 285 and 300 K revealed a network of medium-range NOE connectivities between residues flanking the D-Pro-L-Pro template. A summary of key NOEs observed by NOESY at 285 K are summarized in *Figs. 4* and *5*. The network of NOEs between the Trp[11] side chain on the one side, and Val[1] and Lys[2] on the other (*Fig. 5*), suggests that a stable conformation exists in this part of the molecule. Many of the same NOE connectivities were also found for **1a**,

although as mentioned above, chemical-shift overlap reduced the number of NOEs that could be assigned unambiguously in this molecule. For the residues from Tyr^4 to Asn^8 in **1a** and **1b**, mainly intra- and inter-(neighbouring)-residue NOEs were found, consistent with higher flexibility in this part of the molecule. It is notable that under the same conditions, **2** revealed predominantly intra- and inter-(neighbouring)-residue NOEs, suggesting that stable secondary structure is not present to the same extent as for **1a**,**b**. For this reason, no structure calculations were performed for **2**.

Fig. 4. *NOE Connectivities for* **1b** *from NOESY data*. The NOEs are classified as strong, medium and weak by fat, middle, and thin lines, respectively. Overlap of Glu^{10} NH and Trp^{11} NH resonances precludes observation of this d_{NN} NOE (dotted line). NOEs indicated to ProNH refer instead to the $ProCH_2(\delta)$ protons.

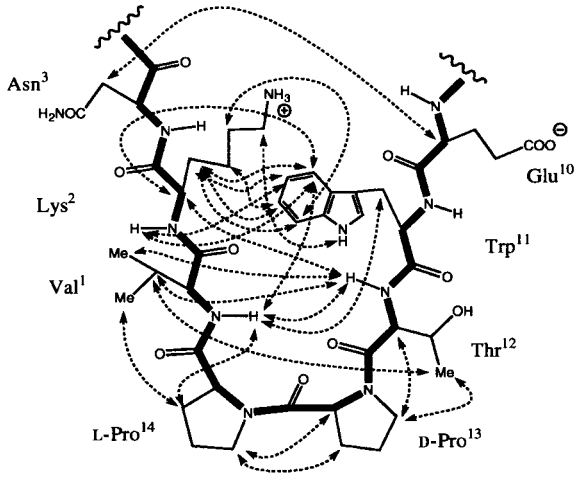

Fig. 5. *Key NOE connectivities for* **1b** *from NOESY data* (dotted lines)

2.2.5. *Structure Calculations.* Average solution structures were calculated for **1b** using dynamic simulated annealing (SA), with upper distance restraints derived from NOESY data. Thirty SA structures were calculated, of which 20 were within 50 kcal/mol and 8 within 25 kcal/mol of the minimum-energy structure. The 8 lowest-energy SA structures could be superimposed with a pairwise r.m.s.d. of 0.46 ± 0.15 Å using the backbone N, C(α) and C atoms of the six residues from Trp^{11}-Thr^{12}-D-Pro^{13}-L-Pro^{14}-Val^1-Lys^2 (*Fig. 6,a*). Several conformers at higher energy had a *cis*-Thr^{12}-D-Pro^{13} peptide bond, but were not considered further, since the NOE data show that all peptide bonds in the major species studied by NMR have the *trans* geometry.

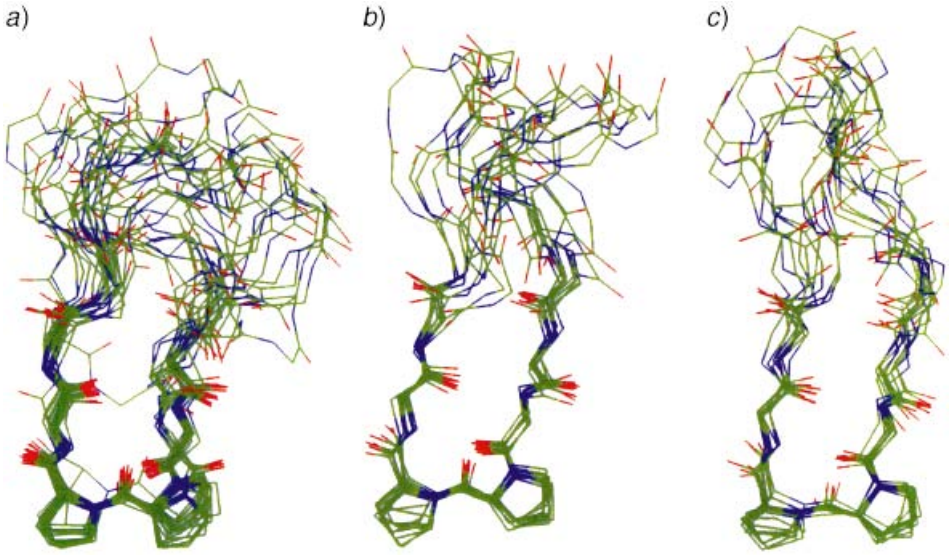

Fig. 6. a) *Superimposition over the backbone N, C(α), and C atoms in residues Trp*[11] *to Lys*[2] *in the 20 lowest-energy structures from simulated annealing of* **1b** (pairwise superimposition r.m.s.d. 0.63 ± 0.27 Å), b) *superimposition over the backbone N, C(α), and C atoms in residues Trp*[11] *to Lys*[2] *of 10 snapshots each taken every 0.2 ns from the MD simulation of* **1b** *with TA-DR* (pairwise superimposition r.m.s.d. 0.46 ± 0.15 Å) *and* c) *superimposition over the backbone N, C(α), and C atoms in residues Trp*[11] *to Lys*[2] *of 10 snapshots each taken every 0.2 ns from the unrestrained MD simulation of* **1b** (pairwise superimposition r.m.s.d. 0.54 ± 0.17 Å). The side chains are omitted for clarity except for D-Pro[13] and Pro[14].

The eight lowest-energy SA structures show only one NOE restraint violation > 0.3 Å within the residues from Trp[11] to Lys[2], whereas the residues from Asn[3] to Glu[10] showed several NOE violations in the range 0.4 – 0.6 Å. For example, the Lys[7] HN to Val[6]-*H*–C(α) restraint was violated in all eight structures, the violation being in the range 0.5 – 0.6 Å. One interpretation of these results is that the residues around the D-Pro-L-Pro template are conformationally ordered in aqueous solution, but the loop residues from Asn[3]-Glu[10] are significantly more mobile, as implied by the superimposition shown in *Fig. 6,a*.

2.2.6. *MD Simulations.* In an attempt to account for conformational averaging in **1b**, the 82 NOE-derived upper distance restraints, and 2 additional H-bonding restraints, were implemented as time-averaged distance restraints [12][13] (TA-DR) in MD simulations at 300 K with explicit water solvent present. The H-bond restraints (Val[1] NH to Thr[12] O, and Thr[12] NH to Val[1] O) were included because the body of data from NH exchange and SA clearly implicate the existence of these interactions. For comparison, an otherwise identical MD simulation was performed without restraints. The starting structure for both simulations was one of the low-energy SA structures having the fewest distance-restraint violations. The most important results of the simulations are given in *Table 4* and *Fig. 6,b* and *c*.

The peptide **1b** undergoes similar dynamical behaviour in both the restrained and unrestrained simulations. This is characterized by relatively small positional fluctua-

Table 4. *Results of the MD Simulation with and without TA-DR for Peptide* **1b**. All averages are over the entire 2-ns simulation.

	Energies [kJ/mol][a])	
	TA-DR	Unrestrained
Potential energy	−77949	−77988
Bond-angle energy	263	258
Improper dihedral energy	77	75
Dihedral energy	127	129
Covalent energy	467	462
Electrostatic energy		
peptide-peptide	−759	−662
peptide-ions	−162	−127
peptide-solvent	−1804	−1978
solvent-solvent	−86634	−86550
LJ interaction energy		
peptide-peptide	−291	−311
peptide-solvent	−290	−281
solvent-solvent	12877	12872
Distance restraint energy	21	–
Temperature [K]	302	302
Sum of violations of distance restraints [Å]	5.7	29.2
Largest violation [Å]	0.8	2.9
Hydrogen bonds (donor/acceptor [%][b]))		
$Val^{1}NH/Thr^{12}O$	79	61
$Asn^{3}NH/Glu^{10}O$	85	36
$Asn^{3}NH/Ser^{9}O$	3	17
$Ser^{9}NH/Asn^{3}O$	7	46
$Glu^{10}NH/Asn^{3}O$	13	<2
$Thr^{12}NH/Val^{1}O$	92	75

[a]) Average contributions to the total energy separated on the basis of terms in the force field [b]) Percentage population of some H-bonds.

tions of the backbone, N, C(α), and C atoms for the six residues Trp^{11} to Lys^{2}, with a significant increase in these fluctuations upon progressing to the tip of the loop, as illustrated in *Fig. 6*,*b* and *c*. The backbone atoms of residues Val^{1}-Lys^{2}-Asn^{3} and Glu^{10}-Trp^{11}-Thr^{12} adopt a typical antiparallel β-sheet geometry (see below). The ϕ/ψ angles for these residues remain in the β-region of the ϕ/ψ space, and the Trp^{11} indole moiety remains close to the Lys^{2} side chain, for almost the entire 2 ns simulation, both with and without restraints. Only the ϕ/ψ angles for Asn^{3} and Glu^{10} show a small degree of fraying outside this β-region. During both simulations, however, the fluctuations in ϕ/ψ angles become more pronounced towards the tip of the loop from Tyr^{4} to Ser^{9}.

In terms of structural mimicry of the receptor loop, of special interest are the residues attached to the template in **1b** (*i.e.*, Val^{1}-Lys^{2} and Trp^{11}-Thr^{12}) and the corresponding residues in the receptor protein. The positions of the peptide-backbone atoms and side chains of these residues in the receptor, as determined crystallographically in two different complexes, one with the ligand IFNγ and the other with the antibody A6 [2][3], are mimicked very closely throughout the restrained and unrestrained MD simulations of **1b** (*Fig. 7*). However, the tip of the loop is clearly more flexible in **1b**, and increased flexibility in this region in the receptor is also

evidenced by the two different loop conformations found in the complexes with A6 and IFNγ [2] [3]. The conformation at the tip of the CC′ loop in the receptor protein will certainly be influenced by the presence of bound protein ligands, when compared to the situation in **1b**. So it is not surprising that the bound conformations at the tip of the CC′ loop observed in the complexes with A6 and IFNγ are not stably reproduced during the simulations of **1b**.

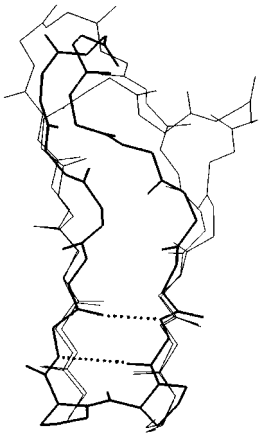

Fig. 7. *Superimposition over the backbone N, C(α), and C atoms in residues Val*^{1}*-Lys*^{2} *and Trp*^{11}*-Thr*^{12} *of one snapshot taken from the MD simulation of* **1b** *with TA-DR* (thick lines) *and the corresponding residues of the CC′ loop of the IFNγR taken from crystal structures of the complexes with A6 and IFNγ* (thin lines). The pairwise superimposition r.m.s.d. was 0.47 ± 0.22 Å. The side chains are omitted for clarity, except for D-Pro^{13} and Pro^{14} in **1b**.

2.3. *Binding Affinities to mAb A6*. Binding studies were undertaken using a surface plasmon resonance (SPR) biosensor (*BIAcore* instrument, *Pharmacia*) to determine the affinities of the peptides to the mAb A6, since the CC′ loop of the receptor appears to comprise a large part of the epitope buried in the A6-receptor complex (*Fig. 1*) [3]. The apparent affinities (K_D) of peptides for A6 were determined in a competitive binding assay [14]; K_D was > 500 μM for **3**, 70 μM for **2**, and 70 μM for **1a**, showing that the linear peptide has essentially no affinity for the antibody, and both cyclic peptides **1a** and **2** have much reduced affinities to A6, in comparison to the intact receptor protein ($K_D \approx 14$ nM) [3]. These results are not surprising, since mutagenesis studies by *Hofstädter* and *Stuart* (unpublished [15]) have shown that Trp^{82} located in the adjacent F strand of the receptor (*Fig. 1*), makes key interactions with the antibody. The replacement of Trp^{82} by alanine leads to a > 2000 fold drop in affinity to the antibody. This interaction with the side chain of Trp^{82} is not provided by the peptides studied here. These results also illustrate one difficulty inherent in attempts to reconstruct a complex conformational epitope in a small molecule mimetic, when key energetic contributions to the functional epitope made by groups far apart in the primary sequence need to be positioned more-or-less precisely at a binding interface. Why is there little difference in the antibody binding affinity between **1a** and **2**, given their different conformational behaviour discussed above? We speculate that this may reflect weak recognition by the antibody (*e.g.*, of charged groups in **1a** and **2**) by mechanisms that are not as sensitive to the conformational dynamics of the peptide backbone.

In those cases where residues in a single β-hairpin loop mediate the energetically important contacts with a ligand or receptor, cyclic peptides constrained by a D-Pro-L-Pro template may prove to be very useful building blocks in mimetic design. Studies are

now underway to establish how effective this approach is, in terms of synthetic efficiency and stabilization of β-hairpin conformations, with loops of diverse sequence and length. In addition, many substituted D- and L-Pro derivatives are available, which may expand considerably the possibilities for constructing new templates based on a D-Pro-L-Pro skeleton.

Experimental Part

General. DMF was dried over $MgSO_4$ and redistilled from ninhydrin. $(i\text{-}Pr)_2EtN$ was redistilled from ninhydrin and KOH just prior to use. HPLC: dual-pump *Pharmacia* system with *Waters RCM-µBondapak*™-C_{18} cartridges (10 µm, 300 Å, 25 × 100 mm) for prep. and (8 × 100 mm) anal. separations, with flow rates of 8 and 2 ml/min, respectively; UV detection at 226 and 278 nm.

*Peptide Synthesis. Cyclo(-Val-Lys-Asn-Tyr-Gly-Val-Lys-Asn-Ser-Glu-Trp-Ile-*D*-Pro-Pro-)* (**1a**) *and Cyclo-(-Val-Lys-Asn-Tyr-Gly-Val-Lys-Asn-Ser-Glu-Trp-Thr-*D*-Pro-Pro-)* (**1b**). Fmoc-Gly-OH (196 mg, 3 equiv.) was linked to *Tentagel-S AC* resin (*Rapp Polymere*, Tübingen) in CH_2Cl_2/pyridine 1:1 (4 ml) using 2-chloro-1,3-dimethylimidazolidinium hexafluorophosphate (370 mg, 6 equiv.) for 1 h. The linear peptide chain was then assembled using standard Fmoc chemistry [9]. The linear dodecapeptide was cleaved from the resin with 1% CF_3COOH in CH_2Cl_2 and purified by HPLC: 306 mg (53%). The linear precursor was cyclized at a concentration of 1 mg/ml in DMF using HATU (1.5 equiv.), HOAt (1.5 equiv.), and $(i\text{-}Pr)_2EtN$ (1% *v*/*v*) for 16 h (see *Fig. 3*). The protected cyclic peptide was purified by HPLC (yield, 82%). Side-chain-protecting groups were removed with CF_3COOH/triisopropylsilane/H_2O 95 : 2.5 : 2.5 for 2 h, and the product was precipitated with Et_2O and purified by HPLC (yield, 77%). EI-MS (**1a**): 1613 (100, $[M+H]^+$). EI-MS (**1b**): 1601 (100, $[M+H]^+$).

Cys-Val-Lys-Asn-Tyr-Gly-Val-Lys-Asn-Ser-Glu-Trp-Ile-Cys (**2**). The linear peptide was assembled on Fmoc-Cys(Trt)-*O*-*p*-alkoxybenzyl alcohol resin (*Bachem*) using standard Fmoc chemistry [9], and cleaved from the resin with CF_3COOH/phenol/H_2O/ethanedithiol 87.5 : 5 : 5 : 2.5. The product was purified by reversed-phase, HPLC (C_{18} column, gradient 20 – 50% MeCN/H_2O + 0.1% CF_3COOH in 20 min). The linear precursor was then strirred in H_2O at pH 8.0 for 14 h. The disulfide-bridged peptide **2** was purified by HPLC under the conditions described above. EI-MS: 821 (100, $[M+2H]^{2+}$).

Glu-Val-Lys-Asn-Tyr-Gly-Val-Lys-Asn-Ser-Glu-Trp-Ile-Asp (**3**). The peptide was assembled on *p*-alkoxybenzyl alcohol resin (*Bachem*) using standard Fmoc chemistry [9], cleaved from the resin with CF_3COOH/phenol/H_2O/triisopropylsilane/ethanedithiol 82.5 : 5 : 5 : 5 : 2.5 and purified by reversed-phase HPLC (C_{18} column, gradient 20 – 40% MeCN/H_2O + 0.1% CF_3COOH in 20 min). EI-MS: 841 (100, $[M+2H]^{2+}$).

NMR, Structure Calculations, and MD Simulations. NOESY, ROESY, TOCSY, and DQF-COSY data were typically obtained for H_2O/D_2O 9 : 1 (pH 5) solns. at 600 MHz (*Bruker AMX600* spectrometer), at a concentration of *ca.* 20 mg/ml. The water signal was presaturated, and 2D spectra were acquired with 2048 × 512 points, except for the determination of coupling constants from E. COSY measured with 8192 × 512 points. NMR Spectra were processed and analysed using *Felix* software (*MSI*, San Diego).

To derive NOE distance restraints, it was assumed that the initial rate approximation is valid and that the peptide rotates as a signal isotropic rotor. The NOE connectivities for **1b** were determined from NOESY with mixing times of 40, 80, 120, and 200 ms. Cross-peak volumes were determined by integration, and the buildup curves were checked to ensure a smooth exponential increase in peak intensity for all NOEs used in deriving distance restraints. The SA calculations were performed with the DISCOVER program (*MSI*, San Diego) and the cvff force field, using a protocol described previously [16].

For the MD simulations with and without TA-DR, the GROMOS96 suite of programs [17] was used, with the 43A1 force field for simulations with solvent water. The 82 NOE-derived upper-distance restraints used were the exact values obtained from NOE buildup curves, with a memory decay time τ_{dr} of 50 ps, and a force constant K_{dr} of 1000 kJ mol^{-1} nm^{-2}. Non-stereospecifically assigned methylene protons were replaced with pseudoatoms, with the necessary distance-restraint correction. The starting structure was a SA structure in a truncated octahedral box (box length 48.42 Å) with 1823 SPC H_2O/molecules, and one Na^+ ion and two Cl^- ions to match the carboxylate side chain of Glu^{10} and the ammonium side chains of Lys^2 and Lys^7 which affords an electrically neutral system. The temperature was held constant by weak coupling (τ_T 0.1 ps) to an external bath at 300 K. The SHAKE algorithm was used to maintain bond lengths with a relative precision of 10^{-4}, and the integrator time step was 0.002 ps. Nonbonded interactions evaluated at every step were within a short-range cut-off of 8 Å. For long-range interactions, the cut-off was 14 Å. Structures were saved for analysis every 100 steps

(0.2 ps). After short simulations to relax the solute and solvent, the simulations with and without TA-DR were each run for 2 ns.

Binding Studies. The *BIAcore-1000* instrument, CM5 sensor chips and surfactant P20 were from *BIAcore AB* (Freiburg, Germany). IFNγR$^{1\text{-}229}$ was prepared as described earlier [3]. PBS buffer (50 mM Na_2PO_4, pH 7.2, 150 mM NaCl) containing 0.005% of surfactant P20 was used as running buffer. Protein and peptide concentrations were calculated from A_{280} measurements after calibration by quantitative amino-acid analysis. Immobilization of mAb A6 on CM5 sensor chips was achieved by random amine coupling. Briefly, the CM5 matrix was activated with a 2 to 4-min injection of 0.08M EDC (*N*-[3-(dimethylamino)propyl]-*N*′-ethyl-carbodiimide)/0.05M NHS (*N*-hydroxysuccinimide), followed by a 4-min injection of mAb A6 (100 µg/ml) in 10 mM NaOAc buffer pH 4.0. Remaining ester groups were blocked by injecting 1M 2-aminoethanol hydrochloride (pH 8.5) for 7 min.

Peptides (final concentration range 10 to 1000 µM) and IFNγR$^{1\text{-}299}$ (80 nM) in PBS buffer were injected (50 µl aliquots) over the A6 surface at a flow rate of 10 µl/min. Bound protein and peptide were removed from a A6 surface by injection of 2-aminoethanol (10 µl, 1.0M, pH 10.0). Injections of IFNγR$^{1\text{-}229}$ alone (80 nM) were performed to ensure that the surface capacity was not significantly altered during the series of experiments. The interactions reached steady state during the sample pulse. The steady-state response (R_{eq}) in the presence and absence of the peptide (the response ratio) can be described by Eqn. 1 [14]; in which $R_{eq,comp} = R_{eq}$ in presence of peptide, $R_{eq,L_1} = R_{eq}$ with receptor alone (80 nM, IFNγR$^{1\text{-}229}$), M_1 = molecular mass of the receptor (27580 Da), M_2 = molecular mass of the peptide, K_1 = affinity constant for the A6-receptor complex [3] ($K_1 = 7.04 \cdot 10^7\ M^{-1}$), K_2 = affinity constant for the A6-peptide complex, c_1 = injected concentration of receptor (80 nM), and c_2 = injected concentration of peptide.

$$\frac{R_{eq,comp}}{R_{eq,L_1}} = \frac{(K_1 \cdot c_1 + M_2/M_1 \cdot K_2 \cdot c_2) \cdot (K_1 \cdot c_1 + 1)}{(K_1 \cdot c_1 + K_2 \cdot c_2 + 1) \cdot K_1 \cdot c_1} \quad (1)$$

Nonlinear fitting of the response ratios and peptide concentration to this equation was performed to derive K_A values ($1/K_D$) for the peptides. The specificity of the competition assay was checked by injecting peptide/receptor mixtures over mAb γR99 immobilized on the sensor chip. This mAb binds an epitope in the second Ig-like domain of the receptor [3] unrelated to that bound by A6. No decrease in receptor binding to γR99 was observed in the presence of the peptides.

The authors thank the *Swiss National Science Foundation* for financial support, Prof. *W. van Gunsteren*, ETH-Z, for the GROMOS96 programs, and Dr. *Fritz Winkler*, *F. Hoffmann-La Roche*, Basel, and Dr. A. Kossiakof, *Genentech*, CA, for crystallographic data of IFNγ-IFNγR complexes.

REFERENCES

[1] B. C. Cunningham, J. A. Wells, *Curr. Opin. Struct. Biol.* **1997**, *7*, 457.
[2] M. R. Walter, W. Windsor, T. L. Nagabhushan, D. J. Lundell, C. A. Lunn, P. J. Zauodny, S. K. Narula, *Nature (London)* **1995**, *376*, 230.
[3] S. Sogabe, F. Stuart, C. Henke, A. Bridges, G. Williams, A. Birch, F. K. Winkler, J. A. Robinson, *J. Mol. Biol.* **1997**, *273*, 882.
[4] J. W. Bean, K. D. Kopple, C. E. Peishoff, *J. Am. Chem. Soc.* **1992**, *114*, 5328.
[5] C. M. Nair, M. Vijayan, Y. V. Venkatachalapathi, P. Balaram, *J. Chem. Soc., Chem. Commun.* **1979**, 1183.
[6] D. K. Chalmers, G. R. Marshall, *J. Am. Chem. Soc.* **1995**, *117*, 5927.
[7] A. B. McElroy, S. P. Clegg, M. J. Deal, G. B. Ewan, R. M. Hagan, S. J. Ireland, C. C. Jordan, B. Porter, B. C. Ross, P. Ward, A. R. Whittington, *J. Med. Chem.* **1992**, *35*, 2582.
[8] P. W. Baures, W. H. Ojala, W. B. Gleason, R. L. Johnson, *J. Pept. Res.* **1997**, *50*, 1.
[9] E. Atherton, R. C. Sheppard, 'Solid Phase Peptide Synthesis – a Practical Approach', IRL Press, Oxford, 1989.
[10] K. Wüthrich, 'NMR of Proteins and Nucleic Acids', J. Wiley & Sons, New York, 1986.
[11] G. Merutka, H. J. Dyson, P. E. Wright, *J. Biomol. NMR* **1995**, *5*, 14.
[12] A. E. Torda, R. M. Scheek, W. F. van Gunsteren, *Chem. Phys. Lett.* **1989**, *157*, 289.
[13] A. P. Nanzer, W. F. van Gunsteren, A. E. Torda, *J. Biomol. NMR* **1995**, *6*, 313.
[14] R. Karlsson, *Anal. Biochem.* **1994**, *221*, 142.

[15] K. Hofstädter, F. Stuart, L. Jiang, J. W. Vrijbloed, J. A. Robinson, *J. Mol. Biol.*, submitted.
[16] C. Bisang, C. Weber, J. A. Robinson, *Helv. Chim. Acta* **1996**, *79*, 1825.
[17] W. F. van Gunsteren, S. R. Billeter, A. A. Eising, P. H. Hünenberger, P. Krüger, A. E. Mark, W. R. P. Scott, I. G. Tironi, 'Biomolcular Simulation: The GROMOS96 Manual and User Guide', Hochschulverlag AG an der ETH Zürich, Zürich, 1996.
[18] R. Koradi, M. Billeter, K. Wüthrich, *J. Mol. Graph.* **1996**, *14*, 51.

Received July 8, 1998